Electronic Supplementary Information

Impact of Charge State on Gas-Phase Behaviors of Noncovalent Protein Complexes in Collision Induced Dissociation and Surface Induced Dissociation

Mowei Zhou†, Shai Dagan‡, Vicki H. Wysocki†*

Department of Chemistry and Biochemistry, University of Arizona, 1306 E. University Blvd., PO Box 210041, Tucson, Arizona

* To whom correspondence should be addressed.

E-mail: wysocki.11@chemistry.ohio-state.edu

† Current address: Department of Chemistry and Biochemistry, Ohio State University, 484 W. 12th Ave., Columbus, Ohio

‡ Permanent address: Israel Institute for Biological Research (IIBR) POB 19, Ness Ziona 74100, Israel

This document includes additional figures that support the discussion in the primary manuscript.

Fig. S1 is an instrument scheme providing technical details.

Fig. S2 is a collection of SID/CID spectra at a variety of collision energies for CRP.

Fig. S3 is a collection of SID/CID spectra at a variety of collision energies for ConA.

Fig. S4 is a CCS plot for CRP pentamer, ConA tetramer and dimer at different charge states.

Fig. S5 is a summary of CCS profiles of remaining undissociated precursors for CRP and ConA, including supercharged precursors.

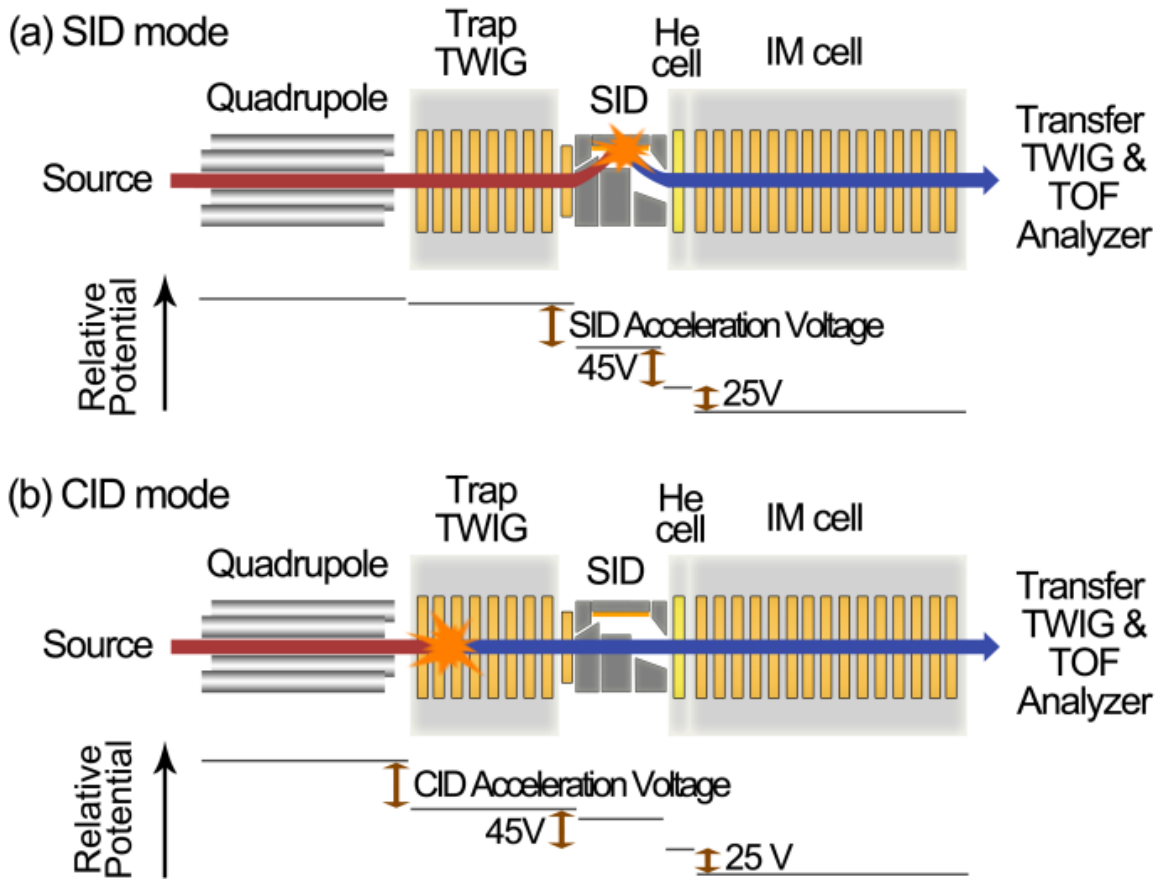

Fig. S1. Ion path and potential diagram of the instrument for (a) SID and (b) CID experiments. Red beam lines indicate precursors, while blue beam lines represent products after CID/SID. The injection voltage for ions entering the pressurized helium cell is 45 V. CID acceleration voltage is defined by the potential difference from the quadrupole to the trap TWIG, while SID acceleration voltage is defined by the potential difference from the trap TWIG to the surface. The potential of the surface is kept 45 V higher than the helium cell in SID experiments, so that the injection voltages for the product ions are the same for CID and SID. The injection voltage from the helium cell into the IM cell is 25 V. A 900 μs delay of the traveling wave in the IM cell was used to ensure that all the ions start IM separation at the same time. No significant differential migration of ions from the trap TWIG release pulse to the entrance of helium cell was observed even at shorter delay times, presumably due to the low pressure and high acceleration in the region. However, the overall drift time is shortened at reduced delay times. Detailed description of the SID device can be found in *Analytical Chemistry* **2012** (84) 6016-6023.

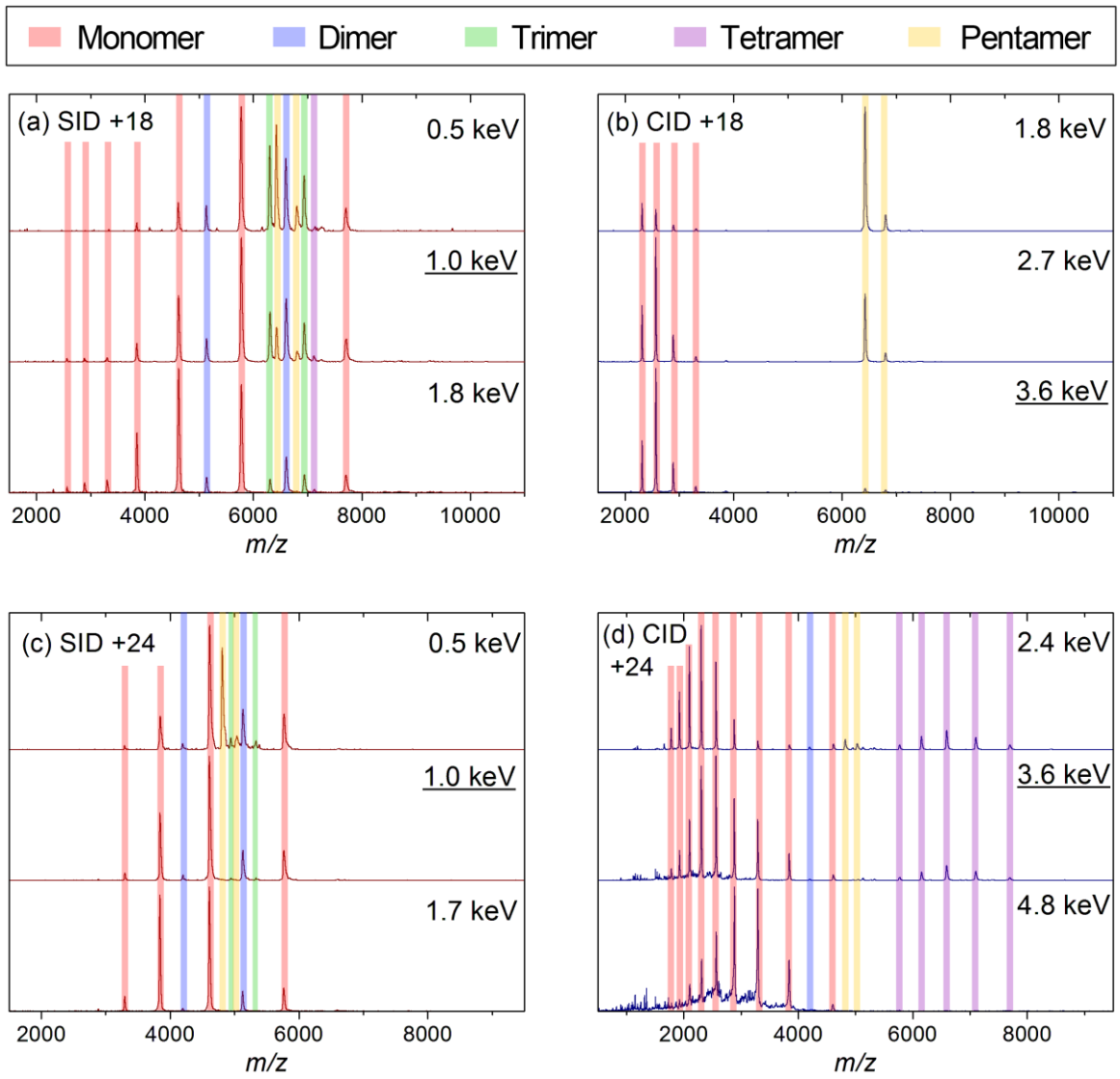

Fig. S2. CID and SID spectra of +18 and +24 CRP at various collision energies. E_{lab} is labeled at the right side of each spectrum. Spectra discussed in the main manuscript are highlighted with E_{lab} underlined. It is noted that some of the peaks constitute of multiple overlapping species. For simplicity, only the major species are labeled in most cases. Generally the spectra do not vary substantially across different collision energies. For CID of both +18 and +24 CRP, the abundance of monomer peaks in low *m/z* region increases at higher collision energies where the precursor is depleted. Additionally, the absence of products in high *m/z* region at 4.8 keV E_{lab} might be attributed to secondary dissociation. The pattern of SID spectra is similar across all collision energies for both precursors, featuring monomer products with lower charge than CID. Likewise, secondary dissociation possibly results in lower abundances of large oligomeric products at higher collision energies.

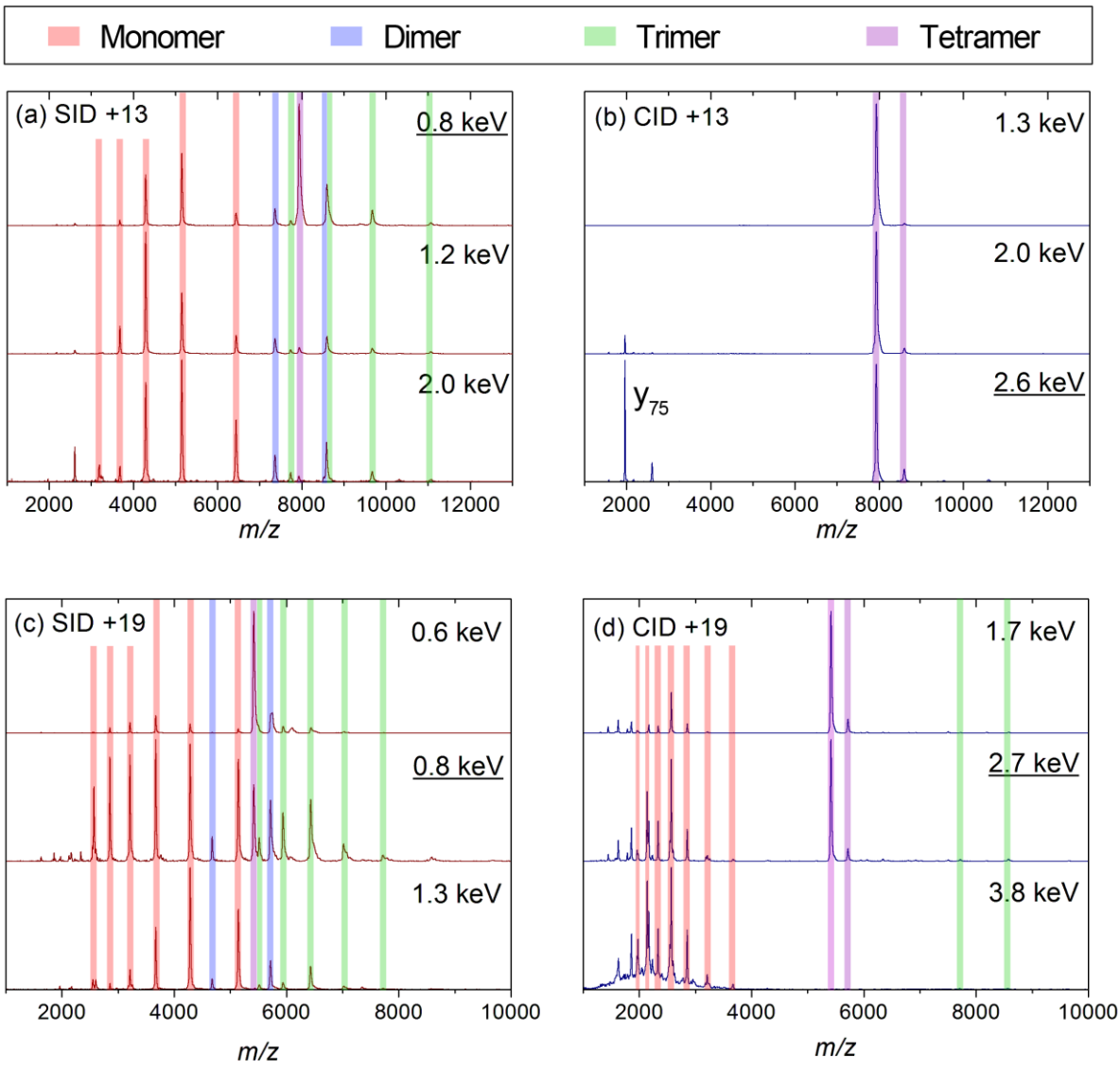

Fig. S3. CID and SID spectra of +13 and +19 ConA at various collision energies. E_{lab} is labeled at the right side of each spectrum. Spectra discussed in the main manuscript are highlighted with E_{lab} underlined. Similarly, the overall dissociation pattern remains the same across different collision energies in all cases. CID spectra of +13 and +19 ConA show exclusively peptide and/or monomer ejection. Instead, SID spectra show mostly dissociation of monomers carrying lower charge than CID products. It is noted that the relative abundance of monomers around 2000 - 4000 *m/z* decreased at higher E_{lab} of 1.3 keV. The shift of distribution to lower charge states indicates that higher energy deposition in SID leads to more dissociation with less unfolding.

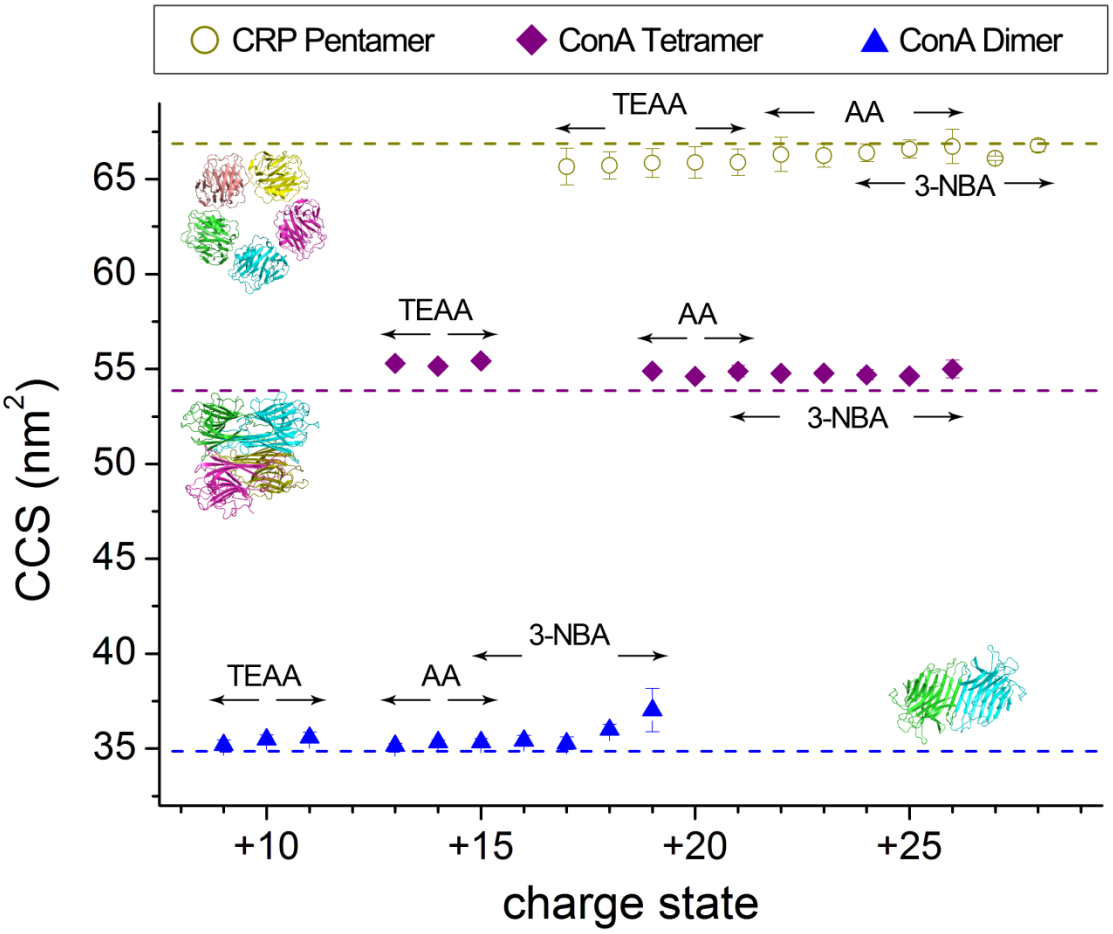

Fig. S4. CCSs of CRP pentamer and ConA tetramer precursors as a function of charge state. ConA dimers in solution equlibrium with ConA tetramers are also included. The buffers used to generate each charge state are labeled beside the data points. Dashed lines are calculated CCSs from crystal structures which are shown as insets. Within the charge states examined, most precursors maintain native-like CCSs as implied by the good agreements with calculated CCSs. ConA dimers show slight increase for charge states higher than +18, suggesting unfolding of the dimers with excess charge.

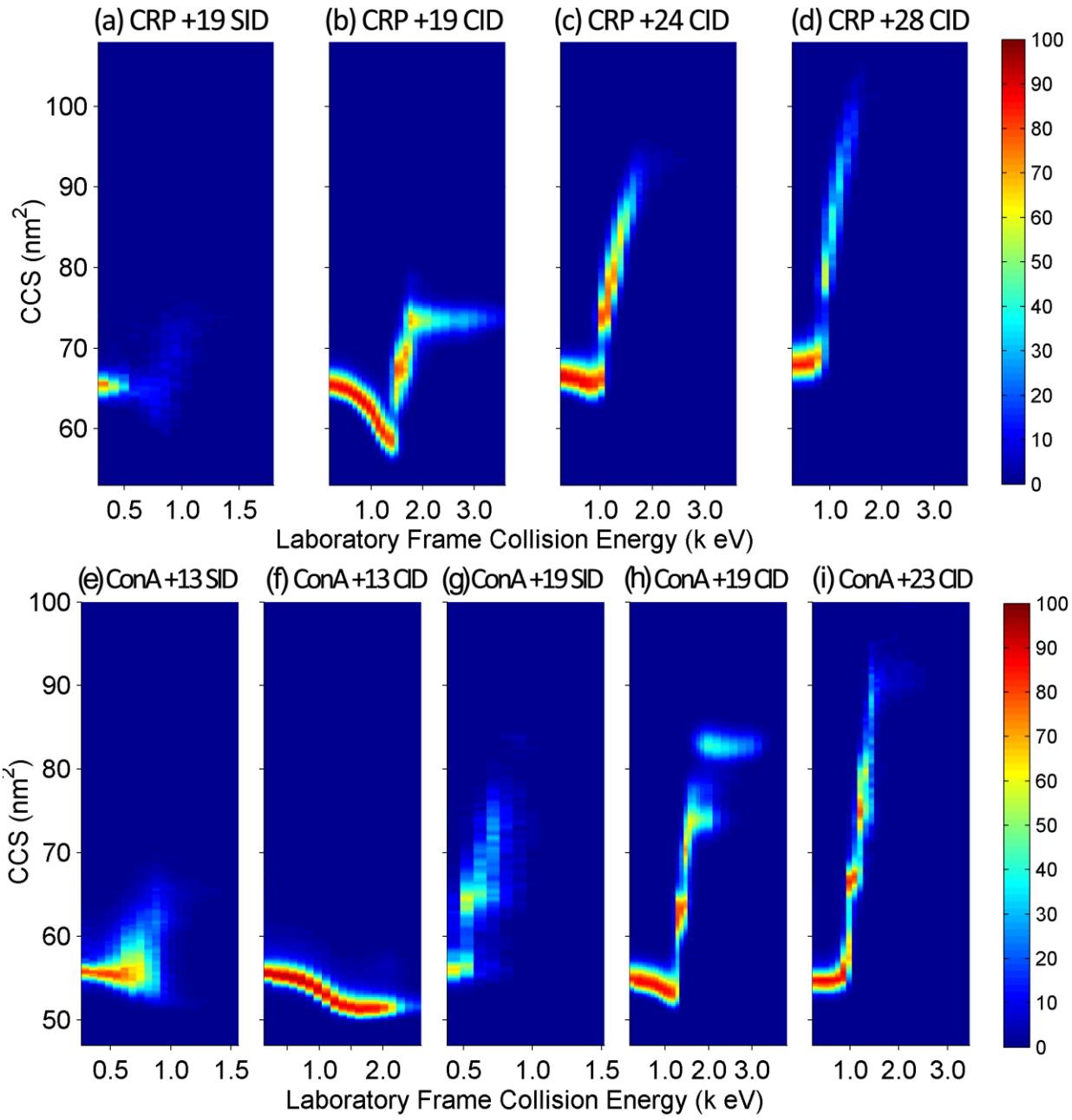

Fig. S5. Summary of CCS change of the remaining precursors upon CID/SID for a variety of charge states of (a-d) CRP and (e-i) ConA, including CID of supercharged precursors (d, i). The same data for the "normal" charged and charge reduced precursors are plotted here for comparison (a-c, e-h). The color scale is shown on the right, indicating the relative abundance of the presursor in the spetra.